ISHAM INTERNATIONAL SOCIETY FOR HUMAN AND ANIMAL MYCOLOGY

Medical Mycology, 2019, 57, S239–S244
doi: 10.1093/mmy/myy140
Review Article

Review Article

Integration of electron microscopy and solid-state NMR analysis for new views and compositional parameters of *Aspergillus fumigatus* biofilms

Courtney Reichhardt[1], Lydia-Marie Joubert[2], Karl V. Clemons[3,4], David A. Stevens[3,4] and Lynette Cegelski[5,*]

[1]Department of Microbiology, University of Washington, Seattle, Washington, USA, [2]Department of Microbiology, Stellenbosch University, Stellenbosch, South Africa, [3]California Institute for Medical Research, San Jose, California USA, [4]Division of Infectious Diseases and Geographic Medicine, Stanford University, Stanford, California, USA and [5]Department of Chemistry, Stanford University, Stanford, California USA

*To whom correspondence should be addressed. Lynette Cegelski, PhD, 380 Roth Way, Keck Building Room 351, Stanford, CA 94304. Tel: 650-725-3527; E-mail: cegelski@stanford.edu

Received 15 August 2018; Revised 25 October 2018; Accepted 24 December 2018; Editorial Decision 5 November 2018

Abstract

The general ability and tendency of bacteria and fungi to assemble into bacterial communities, termed biofilms, poses unique challenges to the treatment of human infections. Fungal biofilms, in particular, are associated with enhanced virulence *in vivo* and decreased sensitivity to antifungals. Much attention has been given to the complex cell wall structures in fungal organisms, yet beyond the cell surface, *Aspergillus fumigatus* and other fungi assemble a self-secreted extracellular matrix that is the hallmark of the biofilm lifestyle, protecting and changing the environment of resident members. Elucidation of the chemical and molecular detail of the extracellular matrix is crucial to understanding how its structure contributes to persistence and antifungal resistance in the host. We present a summary of integrated analyses of *A. fumigatus* biofilm architecture, including hyphae and the extracellular matrix, by scanning electron microscopy and *A. fumigatus* matrix composition by new top-down solid-state NMR approaches coupled with biochemical analysis. This combined methodology will be invaluable in formulating quantitative and chemical comparisons of *A. fumigatus* isolates that differ in virulence and are more or less resistant to antifungals. Ultimately, knowledge of the chemical and molecular requirements for matrix formation and function will drive the identification and development of new strategies to interfere with biofilm formation and virulence.

Key words: *Aspergillus fumigatus*, biofilms, solid-state NMR, electron microscopy.

Introduction

Aspergillus fumigatus is an opportunistic fungus that is the cause of serious human infections including lethal fungal infections among immunosuppressed individuals,[1–3] aspergilloma, and invasive pulmonary aspergillosis.[4,5] *A. fumigatus* is often found together with *Pseudomonas aeruginosa* in lung infections of patients with cystic fibrosis.[6,7] The participation of *A. fumigatus* in biofilm communities specifically contributes to its virulence in invasive pulmonary aspergillosis and aspergilloma.[5] *A. fumigatus* biofilm communities and biofilms in general are assembled from many cells that surround themselves with a self-secreted extracellular matrix of various molecular components, often involving different proteins and polysaccharides as well as sometimes including lipids, nucleic acids and other molecules.[8–10] *A. fumigatus* within biofilm communities exhibits enhanced recalcitrance to antifungal treatment and are implicated in persistent and chronic infections. Thus, interfering with biofilm formation has emerged as an attractive and needed avenue to develop new therapeutics.

Mechanistically, biofilms can be envisioned to protect resident cells from antibiotics through several mechanisms. Physically, the matrix components could prevent antibiotic

penetration to resident cells.[8–11] This could involve chemical sequestering or binding of antifungals by matrix components or repulsion of antifungals due to electrostatic or hydrophobicity considerations.[12,13–18] Biofilm formation also promotes the development of slow-growing persister cells that are not affected by antimicrobials.[19] Efforts to inhibit production of matrix components or to inhibit the physical interactions between secreted components has emerged as an attractive antivirulence approach toward inhibiting biofilm formation and maintaining or enhancing *A. fumigatus* sensitivity to antifungals.[20] Such approaches require knowledge of matrix composition as well as the genetics and molecular mechanisms underlying the regulation and production of the matrix components. These biofilm parameters are not typically available from traditional studies of organisms grown in standard cell culture, in nonbiofilm states.

We have worked to introduce complementary analyses of *A. fumigatus* biofilms to provide holistic views of biofilm architecture and chemical composition.[21,22] For biofilm architecture, we have optimized sample preparation, processing protocols, and visualization using scanning electron microscopy (SEM).[21] Toward obtaining holistic and also chemically specific compositional parameters of intact isolated matrix material, we introduced approaches using solid-state NMR spectroscopy.[22] Solid-state NMR has been employed to obtain compositional and structural detail in complex assemblies including whole bacterial cells and even in intact plant leaves.[23–25] It serves as a powerful complement to traditional biochemical analyses as most biochemical analyses require that the complex and insoluble biofilm matrix be broken down through enzymatic digestion or chemical hydrolysis to generate soluble samples for chromatography, for example, HPLC, and techniques including mass spectrometry and protein gel analysis. Such characterization is crucial for identifying the very specific lists of parts in a complex material. However, matrix materials cannot always be completely solubilized, leaving some material uncharacterized. Also, isolation of specific parts can be accompanied by losses in yield and thus pose a challenge to quantitative analysis of such complex materials. Solid-state NMR analysis of the complex matrix material, on the other hand, can provide a complete accounting of all the types of carbons in a sample and can be applied to nitrogen and phosphorous as well.[26,27] The solid-state NMR spectrum of a matrix sample will not necessarily unambiguously identify the specific proteins or polysaccharides in the sample but will provide quantitative determination of the exact carbon types in a sample, that is, the percent of carbonyls and polysaccharide anomeric carbons and one-bond carbon-nitrogen pairs in a sample. It affords an unambiguous atomic-level chemical accounting that can be used in powerful comparisons across samples.

In exciting examples, we have found this approach of using solid-state NMR on intact matrix samples to also serve as an unanticipated discovery tool. A notable example is our recent discovery that *E. coli* biofilms produce a naturally chemically modified form of cellulose in their biofilm matrix – phosphoethanolamine cellulose.[28,29] Cellulose is the most abundant biomolecule on Earth, and this represents the first discovery of a chemically modified cellulose produced in nature. Standard protocols used to isolate cellulosic materials from biofilms employ harsh acid hydrolysis which we discovered removes the modification.[29] Solid-state NMR spectroscopy can be performed directly on intact biofilms and on the isolated but still insoluble matrix material *in situ*. This work complements proteomics and other biochemical analysis of matrix parts solubilized for standard analytical methods and provides a complete accounting of the various types of molecules to the intact matrix.[21,26–28,30]

We recently reviewed how complementary biochemical and biophysical approaches, including solid-state NMR spectroscopy, generate descriptions of fungal biofilm composition that contribute to drug discovery and development opportunities.[20] Here we focus and provide a summary of the salient features of our analysis of *A. fumigatus* biofilms cultivated in Roswell Park Memorial Institute (RPMI) 1640 medium primarily using scanning electron microscopy and solid-state NMR spectroscopy. Microscopy most obviously provides unique visualization of biofilm architecture. Solid-state NMR parameters, on the other hand, provide compositional boundary conditions—providing a full accounting of all the types of carbons, for example, in a biofilm matrix that can be translated into overall pools of biomolecules such as proteins, lipids and polysaccharides.

A. fumigatus biofilm architecture by SEM

Fungal biofilms consist of a three-dimensional network of cellular hyphae and extracellular matrix. Early electron microscopy work by Beauvais and coworkers, first employing biofilms grown in aerial static cultures, revealed the remarkable global biofilm architecture with ECM covering individual hyphae and serving to glue hyphae together into a contiguous network.[31] Early descriptors even referred to the communities observed *in vivo* as "fungal balls," and these resembled the biofilms assembled in laboratory culture.[31] In addition, this foundational work characterized the matrix composition as containing galactomannan, α1,3 glucans, monosaccharides, polyols, melanin, and proteins.[31] During our own recent work investigating *A. fumigatus* biofilms, we took the opportunity to fully optimize and further explore *A. fumigatus* biofilms and also multispecies interactions through scanning electron microscopy.[21,22]

Visualization of biofilm communities is crucial to understanding biofilm function and, ultimately, to elucidating the mechanisms of inhibitors and the influence of environmental conditions that impact community behavior and, potentially, pathogenesis. We discovered that differences in sample processing and image acquisition parameters differentially emphasize details of different parts of a biofilm.[22] Specifically, some parameters available

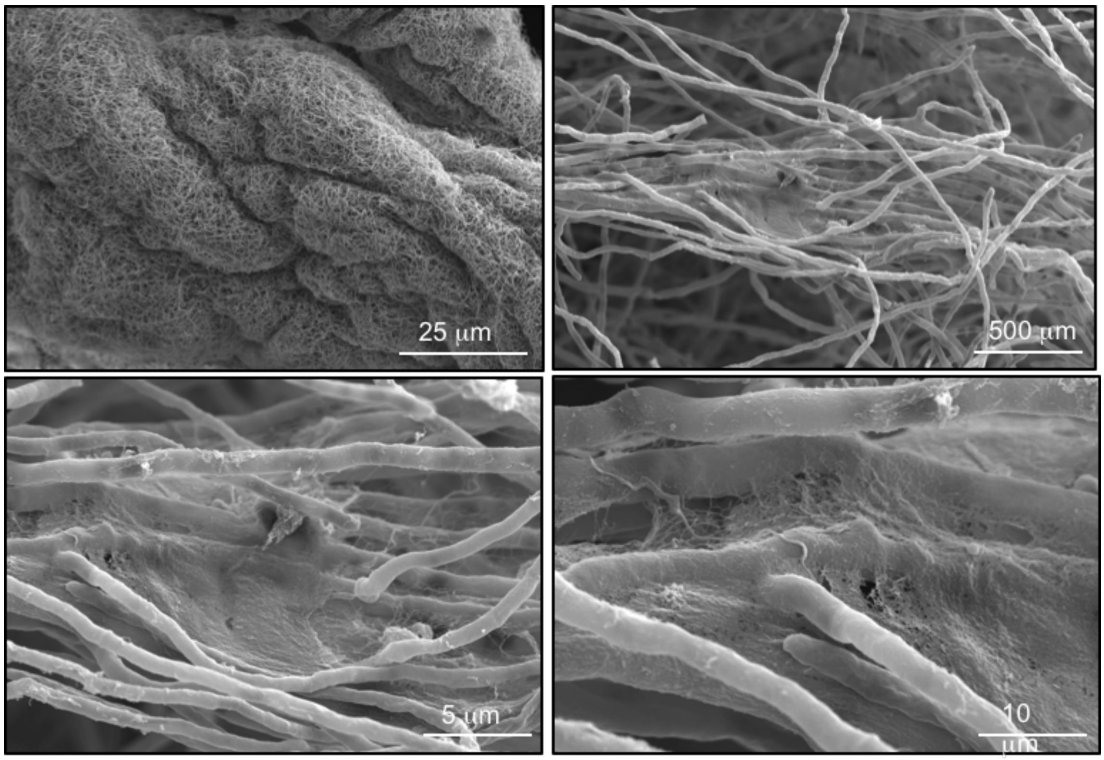

Figure 1. High-resolution ultrastructural SEM analysis of *A. fumigatus* biofilms grown in RPMI 1640 nutrient broth. Micrographs resulted from optimized sample preparation and processing parameters as well as SEM detection methods to enable high-resolution visualization of the fibrous ultrastructure of ECM on and between hyphae. As described previously,[22] samples were harvested from flasks and fixed for limited time periods in 4% paraformaldehyde with 2% glutaraldehyde in 0.1 M sodium cacodylate buffer, rinsed in the same buffer, and post-fixed with 1% OsO4. Samples were then rinsed in water and gradually dehydrated in increasing concentrations of ethanol (50, 70, 90, 100%, 5 min each) and critically point dried with liquid CO_2. Dried samples were sputter-coated (50 Å, Au/Pd) and imaged with a Hitachi S-3400 N SEM operated at 10 kV under high vacuum, using an Everhart-Thornley (ET) SE detector. Top left micrograph reproduced from Joubert et al. 2017.[22] Bottom right micrograph reproduced from Reichhardt et al. 2015.[21]

to an experimenter include aldehyde fixation of samples, heavy metal contrasting, drying techniques, and ionic liquid treatment. Here we present a set of four images obtained with parameters optimized to best capture the ultrastructure of the extracellular matrix material surrounding hyphae (Fig. 1). We note that the ability to resolve the ultrastructural features of cellular and ECM components depended strongly on the fixation and drying techniques and we determined that visualization by high-resolution SEM and field emission SEM techniques using a secondary electron (SE) detector as optimal. Indeed, through our thorough analysis and comparison of many imaging parameters for *A. fumigatus* biofilm, some samples appeared to lack ECM under certain processing and imaging conditions but exhibited surprising quantities of ECM with so-called high-efficiency In-Lens SE detection, which obtains high lateral resolution and edge contrast.[22] The combined results presented a recommendation for achieving consistent high-resolution ultrastructural SEM analysis of cellular features and ECM of *A. fumigatus biofilms* - primarily relying on quite short fixation times and including osmium tetroxide post-fixation, followed by critical point drying.[22]

A. fumigatus biofilm compositional framework from solid-state NMR

We utilized a top-down NMR approach to quantitatively characterize the ECM composition of *A. fumigatus*.[21] This approach uses two types of one-dimensional solid-state NMR experiments: cross-polarization magic-angle spinning (CPMAS) and rotational-echo double-resonance (REDOR) NMR. CPMAS, REDOR, and other solid-state NMR methods have been powerful tools, dating back to 1981, to study chitin-rich materials and fungal cell walls including melanin components.[32–38] The ^{13}C CPMAS spectrum contains information about the quantities of carbon types, including carbonyls, aromatic carbons, and polysaccharide carbons present in the ECM. No ^{13}C labeling was used or needed, and ^{13}C NMR analysis was performed by detecting ^{13}C at natural abundance levels (approximately 1% of all carbons are ^{13}C isotopes). On the other hand, biosynthetic incorporation of ^{15}N labels is required for routine ^{15}N analysis, and ^{15}N was incorporated into cells and the biofilm matrix through use of a fully ^{15}N-labeled version of RPMI 1640 medium. Mature *A. fumigatus* biofilms grown statically in this medium were then subjected to a non-degradative ECM

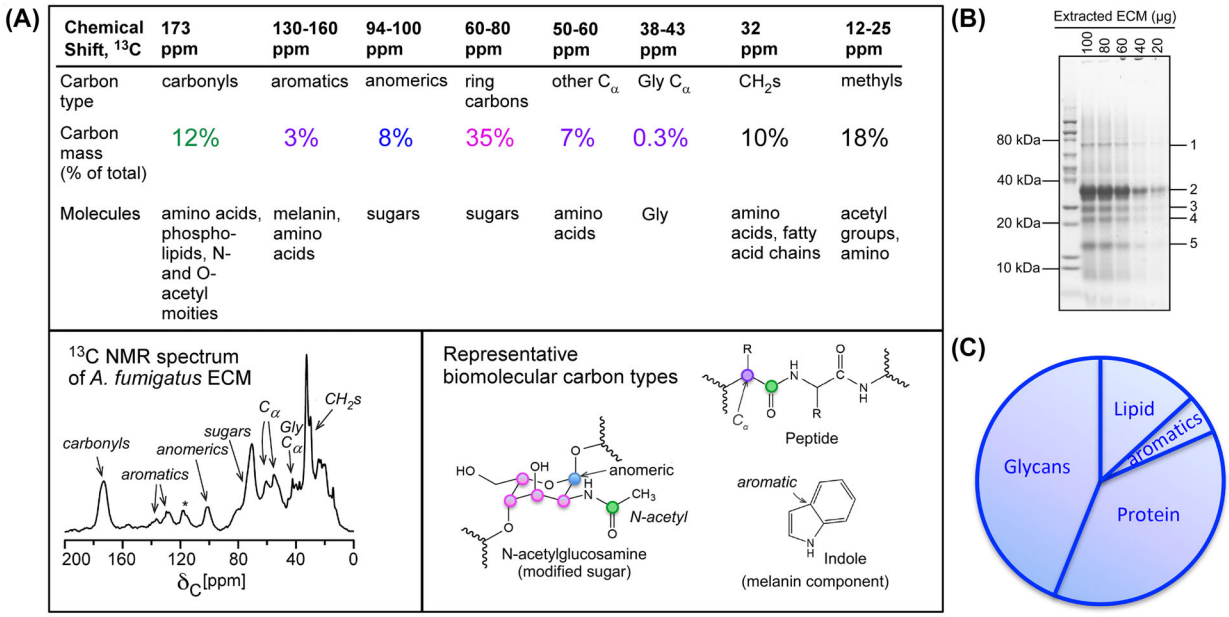

Figure 2. Solid-state NMR measurements provide a quantitative accounting of the chemical composition of the matrix coupled with additional molecular detail from biochemical analysis. (A) Solid-state NMR ^{13}C CPMAS and $^{13}C\{^{15}N\}$REDOR measurements quantify distinguishing carbon pools within the intact extracted *A. fumigatus* ECM. (B) An annotated ^{13}C CPMAS NMR spectrum of the ECM displays the basic spectrum obtained in one CPMAS NMR experiment, wherein the asterisk represents a spinning sideband (reproduced with permission from Reichhardt et al. 2015).[21] Additional experiments were performed to enable integration of carbon contributions and to further quantify carbon types, i.e., specific carbons bonded to nitrogen. (B) Protein gel analysis and protein identification revealed catalase B and Asp f2 as major protein components in the ECM (reproduced from Reichhardt et al. 2015).[21] (C) A Venn diagram summarizes the quantified carbon contributions (percent carbon by mass) in the *A. fumigatus* ECM. This Figure is reproduced in color in the online version of *Medical Mycology*.

extraction protocol.[21] The ^{15}N labeling additionally made it possible to further annotate the carbon pools according to carbon-nitrogen couplings using $^{13}C\{^{15}N\}$REDOR NMR experiments. The ^{13}C CPMAS spectrum of the extracted ECM revealed that the *A. fumigatus* ECM is rich in polysaccharides (Fig. 2A). This was evident as the polysaccharide anomeric carbons (94 to 100 ppm) and associated ring sugar carbons (60 to 80 ppm) accounted for approximately 43% of the total carbon mass. Quantification of contributions to the CPMAS spectrum was enabled with quantitative CP array experiments. A minimum of approximately 5 mg of sample in a 5 mm NMR rotor would be required for this type of NMR analysis with ^{13}C at natural abundance (unlabeled sample). Even smaller samples would be possible in an NMR probe with a smaller diameter coil, for example, 3.2 mm; however, matrix sample amount was not limiting in our application, so rotors of 5 mm or larger are well suited to the measurements. To further annotate the relative contributions of other spectral regions within the ^{13}C spectrum, we used $^{13}C\{^{15}N\}$REDOR as a spectroscopic filter to identify and quantify carbons that are directly bonded to nitrogen. This experiment enabled us to characterize the relative contributions of proteins to the ECM because proteins contain amino acids, each of which has an α-carbon and a carbonyl directly bonded to nitrogen. Through this experiment, we determined that carbonyls (173 ppm) account for 12% of the total carbon mass. Similarly, we determined that α-carbons (50 to 60 ppm) are 7% of the total carbon mass. The stoichiometric excess of carbonyls relative to α-carbons can be attributed to lipids and modifications on sugars, for example, acetyl groups. Interestingly, from the ratio of polysaccharide anomeric carbons (8%) to α-carbons (7%), even in the absence of other information and ^{15}N NMR experiments, one can quickly estimate that the percentages of polysaccharides and protein in the ECM are approximately equal as stoichiometrically there is one anomeric carbon per sugar unit and one α-carbon per amino acid. The results of the full analysis are displayed in Figure 2A.

To identify the specific protein components within the *A. fumigatus* ECM, we applied more traditional biochemistry methods. Specifically, we analyzed the ECM using SDS-PAGE paired with mass spectrometry and Edman sequencing for protein identification (Fig. 2B). Although this method only detects SDS soluble proteins, it is still useful to help characterize the ECM. By SDS-PAGE analysis, the ECM contained several SDS-soluble proteins. Five bands corresponding to high abundance ECM proteins (labeled 1–5) were examined by mass spectrometry and Edman degradation. Two unique proteins, catalase B (band 1; M.W. 79,910 Da) and Asp f2 (band 2; M.W. 32,838 Da), were identified. Both catalase B and Asp f2 are known to be secreted from the cells, and are *N*-linked glycosylated.[39–41] Through further analysis that included treatment of the ECM with peptide-*N*-glycosidase F (PNGase), we determined that bands 3, 4, and 5 correspond to deglycosylated and truncated forms of catalase

B and Asp f2. Thus, the major protein components of the ECM were attributed to catalase B and Asp f2.[21]

In summary, using the combination of CPMAS and the selective recoupling experiment, $^{13}C\{^{15}N\}$REDOR, we provided a quantitative categorization of all carbons in the ECM (Fig. 2C). We further identified ECM proteins using more traditional biochemistry methods. The future benefit of elucidating the ECM composition in this way is two-fold. First, we now have a means of tracking changes in composition due to drug treatment or changes in environment, and in a way that does not rely on solubilizing ECM with caveats regarding incomplete sample dissolution and ambiguities on quantitative contributions based on what can be solubilized and analyzed. Second, we can apply this integrated methodology to determine the composition of other types of biofilm. Together with the invaluable visualization of *Aspergillus* biofilms by electron microscopy, we are excited by the possibilities of connecting specific parameters of biofilm matrix composition with function and guiding the understanding and development of antifungals and biofilm inhibitors with new modes of action.

Acknowledgments

L.C. acknowledges support from the National Science Foundation CAREER Award 1453247. K.V.C. and D.A.S. acknowledge support from the John Flatley Foundation (CIMR grant # 3-770). C.R. is a recipient of the Carol Basbaum Memorial Research Fellowship, Cystic Fibrosis Foundation.

Declaration of interest

The authors report no conflicts of interest. The authors alone are responsible for the content and the writing of the paper.

References

1. Douglas LJ. *Candida* biofilms and their role in infection. *Trends Microbiol*. 2003; 11: 30–36.
2. Mayer FL, Wilson D, Hube B. *Candida albicans* pathogenicity mechanisms. *Virulence*. 2013; 4: 119–128.
3. Mowat E, Williams C, Jones B, Mcchlery S, Ramage G. The characteristics of *Aspergillus fumigatus* mycetoma development: is this a biofilm? *Med Mycol*. 2009; 47: S120–126.
4. Balajee SA, Houbraken J, Verweij PE et al. *Aspergillus* species identification in the clinical setting. *Stud Mycol*. 2007; 59: 39–46.
5. Kaur S, Singh S. Biofilm formation by *Aspergillus fumigatus*. *Med Mycol*. 2014; 52: 2–9.
6. Bakare N, Rickerts V, Bargon J, Just-Nubling G. Prevalence of *Aspergillus fumigatus* and other fungal species in the sputum of adult patients with cystic fibrosis. *Mycoses*. 2003; 46: 19–23.
7. Manavathu EK, Vager DL, Vazquez JA. Development and antimicrobial susceptibility studies of *in vitro* monomicrobial and polymicrobial biofilm models with *Aspergillus fumigatus* and *Pseudomonas aeruginosa*. *BMC Microbiol*. 2014; 14: 53–68.
8. Flemming HC, Wingender J. The biofilm matrix. *Nat Rev Microbiol*. 2018; 8: 623–633.
9. Flemming HC, Neu TR, Wozniak DJ. The EPS matrix: the "house of biofilm cells". *J Bacteriol*. 2007; 189: 7945–7947.
10. Blankenship JR, Mitchell AP. How to build a biofilm: a fungal perspective. *Curr Opin Microbiol*. 2006; 9: 588–594.
11. Mathe L, Van Dijck P. Recent insights into *Candida albicans* biofilm resistance mechanisms. *Curr Genetics*. 2013; 59: 251–264.
12. Al-Fattani MA, Douglas LJ. Biofilm matrix of *Candida albicans* and *Candida tropicalis*: chemical composition and role in drug resistance. *J Med Microbiol*. 2006; 55: 999–1008.
13. Donlan RM, Costerton JW. Biofilms: survival mechanisms of clinically relevant microorganisms. *Clin Microbiol Rev*. 2002; 15: 167–193.
14. Al-Fattani MA, Douglas LJ. Penetration of *Candida* biofilms by antifungal agents. *Antimicrob Agents Chemother*. 2004; 48: 3291–3297.
15. Lewis K. Riddle of biofilm resistance. *Antimicrob Agents Chemother*. 2001; 45: 999–1007.
16. Taff HT, Nett JE, Zarnowski R et al. A *Candida* biofilm-induced pathway for matrix glucan delivery: implications for drug resistance. *PLoS Path*. 2012; 8: e1002848.
17. Ramage G, Rajendran R, Sherry L, Williams C. Fungal biofilm resistance. *Int J Microbiol*. 2012; e528521.
18. Mukherjee PK, Chandra J. *Candida* biofilm resistance. *Drug Resist Updat*. 2004; 7: 301–309.
19. Lewis K. Persister cells, dormancy and infectious disease. *Nat Rev Microbiol*. 2007; 5: 48–56.
20. Reichhardt C, Stevens DA, Cegelski L. Fungal biofilm composition and opportunities in drug discovery. *Future Med Chem*. 2016; 8: 1455–1468.
21. Reichhardt C, Ferreira JA, Joubert LM, Clemons KV, Stevens DA, Cegelski L. Analysis of the *Aspergillus fumigatus* biofilm extracellular matrix by solid-state nuclear magnetic resonance spectroscopy. *Eukaryot Cell*. 2015; EC–00050.
22. Joubert LM, Ferreira JA, Stevens DA, Nazik H, Cegelski L. Visualization of *Aspergillus fumigatus* biofilms with scanning electron microscopy and variable pressure-scanning electron microscopy: a comparison of processing techniques. *J Microbiol Methods*. 2017; 132: 46–55.
23. Romaniuk JAH, Cegelski L. Bacterial cell wall composition and the influence of antibiotics by cell-wall and whole-cell NMR. *Phil Trans R Soc B*. 2015; 370: 20150024.
24. Toke O, Cegelski L. REDOR applications in biology: an overview. In *Solid State NMR Studies of Biopolymers*. Chichester: John Wiley & Sons, 2010: 473–490.
25. Cegelski L. REDOR NMR for drug discovery. *Bioorg Med Chem Lett*. 2013; 23: 5767–5775.
26. Reichhardt C, Cegelski L. Solid-state NMR for bacterial biofilms. *Mol Physics*. 2014; 112: 887–894.
27. Cegelski L. Bottom-up and top-down solid-state NMR approaches for bacterial biofilm matrix composition. *J Magn Resonan*. 2015; 253: 91–97.
28. McCrate OA, Zhou X, Reichhardt C, Cegelski L. Sum of the parts: composition and architecture of the bacterial extracellular matrix. *J Mol Biol*. 2013; 425: 4286–4294.
29. Thongsomboon W, Serra DO, Possling A, Hadjineophytou C, Hengge R, Cegelski L. Phosphoethanolamine cellulose: a naturally produced chemically modified cellulose. *Science*. 2018; 359: 334–338.
30. Reichhardt C, Fong JC, Yildiz F, Cegelski L. Characterization of the *Vibrio cholerae* extracellular matrix: a top-down solid-state NMR approach. *Biochim Biophys Acta*. 2015; 1848: 378–383.
31. Beauvais A, Schmidt C, Guadagnini S et al. An extracellular matrix glues together the aerial-grown hyphae of *Aspergillus fumigatus*. *Cell Microbiol*. 2007; 9: 1588–1600.
32. Zhong J, Frases S, Wang H, Casadevall A, Stark RE. Following fungal melanin biosynthesis with solid-state NMR: biopolymer molecular structures and possible connections to cell-wall polysaccharides. *Biochem*. 2008; 47: 4701–4710.
33. Chatterjee S, Prados-Rosales R, Frases S, Itin B, Casadevall A, Stark RE. Using solid-state NMR to monitor the molecular consequences of Cryptococcus neoformans melanization with different catecholamine precursors, *Biochem*. 2012; 51: 6080–6088.
34. Chatterjee S, Prados-Rosales R, Itin B, Casadevall A, Stark RE. Solid-state NMR reveals the carbon-based molecular architecture of *Cryptococcus neoformans* fungal eumelanins in the cell wall. *J Biol Chem*, 2015; 290: 13779–13790.
35. Schaefer J, Kramer KJ, Garbow JR et al. Aromatic cross-links in insect cuticle: detection by solid-state 13C and 15 N NMR. *Science*. 1987; 235: 1200–1204.
36. Fukamizo T, Kramer KJ, Mueller DD, Schaefer J, Garbow J, Jacob GS. Analysis of chitin structure by nuclear magnetic resonance spectroscopy and chitinolytic enzyme digestion. *Arch Biochem Biophys*. 1986; 249: 15–26.

37. Duarte ML, Ferreira MC, Marvao MR, Rocha J. Determination of the degree of acetylation of chitin materials by 13C CP/MAS NMR spectroscopy. *Inter J Biol Macromol*. 2001; 28: 359–363.
38. Kang X, Kirui A, Muszyński A et al. Molecular architecture of fungal cell walls revealed by solid-state NMR. *Nat Comm*. 2018; 9: 2747.
39. Zarnowski R, Westler WM, Lacmbouh GA et al. Novel entries in a fungal biofilm matrix encyclopedia. *mBio*. 2014; 5: e01333–01314.
40. Oda K, Kakizono D, Yamada O, Iefuji H, Akita O, Iwashita K. Proteomic analysis of extracellular proteins from *Aspergillus oryzae* grown under submerged and solid-state culture conditions. *Appl Environ Microbiol*. 2006; 72: 3448–3457.
41. Banerjee B, Greenberger PA, Fink JN, Kurup VP. Immunological characterization of Asp f2, a major allergen from *Aspergillus fumigatus* associated with allergic bronchopulmonary aspergillosis. *Infect Immun*. 1998; 66: 5175–5182.